

Anti Microbial, Anti Oxidant and Anticancer Activity of La/Bi/Cu Trimetal/Chitosan Nanocomposites

P. GURULAKSHMI *¹, JESSICA FERNANDO ²

¹Research Scholar (Reg.No: 19122232032011), PG and Research Department of Chemistry, V.O.Chidambaram College, Thoothukudi, India(Affiliated to ManonmaniamSundaranar University, Abishekapatti,Tirunelveli)

¹Assistant Professor, PG&Research Department of Chemistry, A. P. C. Mahalaxmi College for Women, Thoothukudi.

²Assistant Professor,PG &Research Department of Chemistry,V.O.Chidambaram College, Thoothukudi, India (Affiliated to ManonmaniamSundaranar University, Abishekapatti,Tirunelveli)

(Corresponding author E-mail: guru199127@gmail.com)

ABSTRACT

Chitosan has been reported to be an effective chelating or fixing agent due the number of NH₂ and OH groups, high adhesion and mechanical strength. It has wide potential applications,especially in drug delivery. In the present study, we report the facile synthesis of La/Bi/Cu /chitosan nanocomposites and their physical properties. La/Bi/Cu trimetal nanoparticles were synthesized by chemical reduction of corresponding metal salts with NaBH₄ in the presence of chitosan, when chitosan molecules adsorb on to the surface of as-prepared La/Bi/Cu trimetal nanoparticles forming La/Bi/Cu /Chitosan nanocomposites. Natural chitosan not only acts as supporting matrix, but also serves as a stabilizer for the formation ofLa/Bi/Cu trimetal nanoparticles. La/Bi/Cu /Chitosan nanocomposites have better antioxidant activity.La/Bi/Cu /Chitosan nanocomposites acts as better antimicrobial activity against bacteria and fungus. La/Bi/Cu /Chitosan nanocomposites have cytotoxic activity against HOS cell line. The optical properties, morphologies, structure, chemical compositions and electronic properties of La/Bi/Cu /chitosan composites were characterized by XRD, FTIR, SEM and UV-visible absorption spectroscopy. The SEM images showed variation in morphology of the particles. The XRD pattern revealed the crystalline nature of the nanocomposites.

Keywords: Trimetal, Chitosan, Anticancer, Anti bacterial and Anti fungal.

INTRODUCTION

More than adequate examination has been done and written about new metal-natural nanocomposites¹. The term nanocomposite as a rule alludes to polymers with scattered nanofillers with a normal molecule size of under 100 nm². Polymers are viewed as great receptors for metals^{3,4} and semiconductor nanoparticles⁵⁻⁷, notwithstanding their incredible optical and electrical properties. It has been accounted for that an enormous number of polymer-inorganic nanocomposites as a rule have alluring electrical, optical and attractive properties that are better than those of the parent polymer or inorganic particles^{8,9}. As a rule, metal nanoparticle-polymer nanocomposites can be ready by adding a metal forerunner to a polymer arrangement and afterward lessening the metal antecedent with a diminishing specialist or pyrolysis specialist, or by adding the metal antecedent through additional decrease or polymerization during polymerization.

In the age of metal nanoparticles, stabilizers assume a significant part in controlling the development and soundness of nanoparticle scattering. Polymers have additionally been utilized to make metallic polymer nanocomposites. Chitosan is a biodegradable, non-poisonous and biocompatible polymer got from a wellspring of somewhat deacylated chitin.¹⁰ Chitosan can be utilized as a compelling fixing specialist for metal nanoparticles (NPs) because of the huge measure of NH₂-and OH-in the compound construction of chitosan^{11,12}. Chitosan is much of the time utilized as a substrate or scattering transporter as a result of its great grip, high hydrophilicity, great film-framing capacity, and high mechanical strength¹³⁻¹⁵. Moreover, dynamic amino and hydroxyl utilitarian gatherings can give reactant materials in improved yields. Chitosan additionally gives phenomenal film development, great bond, minimal expense, non-poisonousness, high mechanical strength, and hydrophilicity.¹⁶ Several writers have shown that chitosan is a functioning transporter for use in the sythesis and catalysis of metal

nanoparticles¹⁷. For instance, it was found that bio-conjugated Ag-chitosan and Au-chitosan show synergist movement in the decrease of nitro sweet-smelling compounds¹⁸.

MATERIALS AND METHODS

Materials

All the chemicals used in this experiment were obtained from Sigma Aldrich chemicals India. Double distilled water was utilized for all processes. Filtration was done using Whatman no.1 filter papers. Glasswares used for the reactions were washed well, rinsed with double distilled water and dried in hot air oven.

Synthesis of La/Bi/Cu /Chitosan Nanocomposites

In a typical synthesis protocol, 10ml of 0.01M lanthanum nitrate, bismuth nitrate and copper nitrate was added and stirred using a magnetic stirrer. After 15mins 5mL of 0.01M NaBH₄ was added drop wise to the solution with constant stirring. The colour of the solution changed from light green to dark brown, which indicated the formation of trimetal nanoparticles. Then, 50 ml of 0.5% (w/v) chitosan solution (prepared using 0.1% acetic acid) was added to trimetal nanoparticles. The solution in the beaker was stirred in a magnetic stirrer at 80° C for about 5 hours. The synthesized La/Bi/Cu /chitosan nanocomposites was washed with water and ethanol to remove unreacted precursor and impurities, and dried to get powdered nanocomposite. Similar procedure was repeated for synthesis of different compositions, ie., (1% (w/v) chitosan, 2% (w/v) chitosan, 3% (w/v) chitosan, 4% (w/v) chitosan) La/Bi/Cu /Chitosan Nanocomposites.

Characterization

UV-Vis spectral analysis was performed on a JASCO-V-600 spectrophotometer at SFR College, Sivakasi. SEM was recorded in MIRA3 TESCAN instrument, EDX at Karunya University, Coimbatore. XRD was recorded using monochromatic Cu K α radiation with a wavelength of 1.54Å at Karunya University, Coimbatore.

Antifungal Assay

Antibiotic susceptibility tests were determined by agar disc diffusion (Kirby-Bauer) method. Fungi strains *Aspergillus niger*, *Aspergillus flavus*, *Candida albicans* and *Aspergillus terreus* were swabbed using sterile cotton swabs in SDA agar plate. 10 μ L of each sample (1,2,3 and 4) was respectively introduced in the sterile discs using sterile pipettes. The disc was then placed on the surface of SDA medium and the compound was allowed to diffuse for 5 minutes and the plates were kept for incubation at 22°C for 48 hours. At the end of incubation, inhibition zones were examined around the disc and measured with transparent ruler in millimeters.

Evaluation of Antibacterial activity

Antibacterial activity of the trimetal nanoparticles were examined using water as solvent and tested against four different human pathogens such as *Bacillus* sp. 1.3, *Bacillus* sp. 8.5, *Pseudomonas aeruginosa*, *Enterobacter cloacae* using agar well diffusion method [22]. The sterilized media are cooled to around 50°C and poured into petriplates which are covered immediately. Nutrient agar plates were swabbed (sterile cotton swabs) with 12 hour old - broth culture of respective bacteria. Wells were made in each of these plates using sterile cork borer (8mm diameter). Trimetal nanoparticles of different concentrations from 100mg/ml to 300mg/ml were prepared. About 30 μ l of different concentrations of trimetal nanoparticles were

added using sterile pipettes into the wells and allowed to diffuse at room temperature for 2 hrs. The plates were incubated at 37°C for 18-24 h. The diameter of the inhibition zone (mm) was measured.

Evaluation of antioxidant activity

The DPPH radical scavenging activity is generally quantified in terms of inhibition percentage of the pre-formed free radical by antioxidants, and the EC₅₀ (concentration required to obtain a 50% antioxidant effect) is a typically employed parameter to express the antioxidant capacity and to compare the activity of different compounds. To evaluate this method, we investigated the antioxidant activity nanoparticles with different concentrations. For this project, ascorbic acid was screened as antioxidant standards with DPPH assay to define the EC₅₀ parameters (Chen et al., 2013).

5mg of standard (Ascorbic acid) was dissolved in 1ml methanol, from this mixture 200µl was taken and diluted in 10ml methanol. The final working concentration of standard was 1mg/10 ml and the sample concentration was 1mg/ml. The standard concentration with four different ranges from 2.5µl, 5µl, 7.5µl and 10µl and sample concentration with 5 different concentrations 10µl, 20µl, 40µl, 80µl and 100µl. The standard, DPPH, and samples were dissolved in 100% methanol.

To assess the free radical scavenging activity of nanoparticles, 1,1-diphenyl-2-picrylhydrazyl (DPPH) assay was performed. Different concentrations of nanoparticles reacted with 100 µL of 0.2 mM DPPH ethanol solution and ascorbic acid was used as an antioxidant reference. The solution was incubated at 37°C in dark for 30 min and the absorbance samples (A_{sample}) were measured at 517 nm against a blank (Methanol alone) and a control solution (A_{control}) with 0.2 mM DPPH and distilled water.

The DPPH free-radical scavenging activity was calculated as follows:

$$\text{Radical scavenging activity (\% RSA)} = \frac{(A_{\text{control}} - A_{\text{sample}})}{(A_{\text{control}})} \times 100$$

The positive controls were those used as the antioxidant reference. By using linear regression of plot the EC₅₀ value was calculated.

Anticancer activity in (ATCC CRL-1543) cell line (Human Osteosarcoma cells – HOS cells)

The HOS cells cultured in Eagle's Minimum Essential Medium with 10% fetal bovine serum were subculture in flat bottomed plates at 5×10^4 cells/well in 100µl culture medium. Different concentration of given samples (10, 20, 40, 60, 80 and 100 µl/ml) was added to the cells and incubated overnight at 37°C in the CO₂ incubator. The HOS cells were observed under microscope and photographed. After incubation, 50µl of MTT solution was added and further incubated for 3 hours. Then, 150 µl of the solubilisation solution was added into each well, wrapped with aluminum foil and incubated 15 mins. The absorbance of the resultant formazan product was measured at 570 nm in the spectrophotometer.

Results and Discussion

UV- Vis spectra of synthesized La/ Bi /Cu /Chitosan Nanocomposites

Formation of La/ Bi /Cu /Chitosan Nanocomposites was confirmed by UV-Vis spectral analysis. UV-Vis spectra of synthesized La/Bi/Cu /Chitosan Nanocomposites is shown in fig.1.

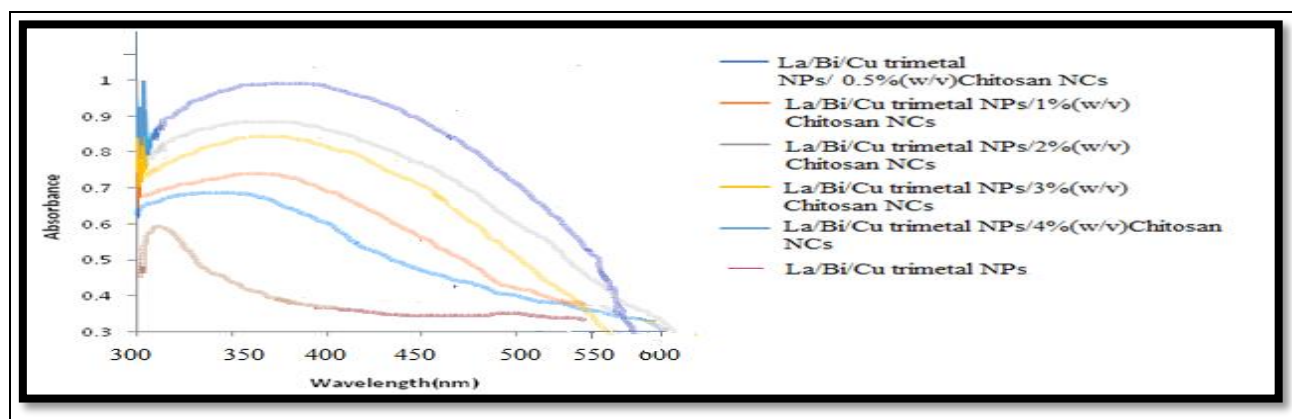


Fig.1: UV- Vis spectra of La/ Bi /Cu /Chitosan Nanocomposites

Absorbance at 308 nm is due to the formation of La/ Bi /Cu trimetal NPs. SPR band around 350-600 nm is observed which shows La/ Bi /Cu /Chitosan Nanocomposites formed. Since the exact position of the SPR band is not known, it is determined by certain parameters such as the capping agent, the size and shape of the nanoparticles^{19,20}. When the concentration of chitosan is increased, the intensity of the absorption band increases as shown in Fig. 1. At the same time, the absorption band at 310 nm of La/ Bi /Cu trimetal NPs becomes broader for La/ Bi /Cu /Chitosan Nanocomposites as chitosan concentration increases. This indicates that the size of trimetal nanoparticles formed altered as the interaction with chitosan increases, which operates as a controller of nucleation as well as a stabilizer²¹.

FTIR spectra of synthesized La/ Bi /Cu /Chitosan Nanocomposites

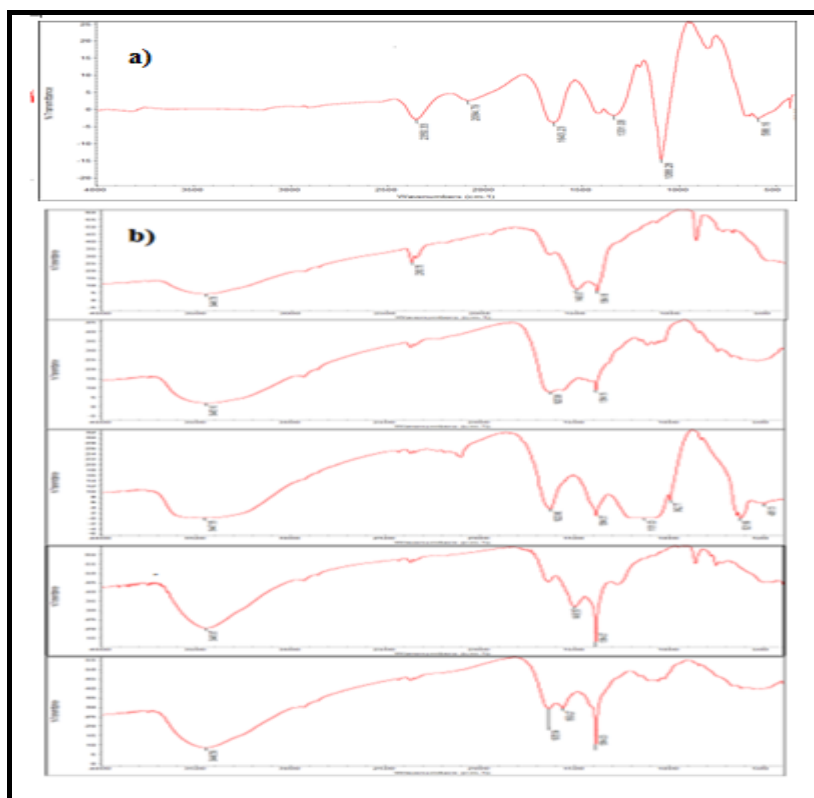


Fig.2. FTIR spectra of a) Chitosan, b) La/ Bi /Cu /Chitosan Nanocomposites at different concentration (0.5% (w/v) , 1.0% (w/v) , 2.0% (w/v) , 3.0% (w/v) , 4.0% (w/v)) of Chitosan

Table-1: Frequency Data of FTIR Spectrum of Trimetal Nanoparticle and Trimetal/Chitosan Nanocomposites

Wavenumber(cm^{-1})						Functional group(s)
La/Bi/Cu Trimetal nanoparticles	La/ Bi /Cu trimetalNPs /0.5% Chitosan NC	La/ Bi /Cu trimetal NPs /1% (w/v) Chitosa n NC	La/ Bi /Cu trimetal NPs /2% (w/v) Chitosa n NC	La/ Bi /Cu trimetal NPs /3% (w/v) Chitosa n NC	La/ Bi /Cu trimetal NPs /4% (w/v) chitosa n NC	
-	3446	3445	3447	3444	3445	O-H Stetching
2350	2360	-	-	-	-	C-H Stetching
1331	1490	1493	1384	1384	1384	C-H bending
-	1184	1132	1131	1134	1154	C-N plane bending
-	930	994	992	998	996	C-O ring of polysaccharides
588	595	623	621,495	653	634	M-C Stretching

The FTIR measurement of La/ Bi /Cu trimetal NPs and La/ Bi /Cu /Chitosan Nanocomposites with different composition are shown in Fig 2a and 2b respectively. FTIR analysis is used to identify the presence of capping agents and stabilizers in the polymer. The peak around 3300 cm^{-1} , corresponds to O-H stretch of hydroxyl groups of chitosan²². This peak is shifted to around 3445 cm^{-1} which may be due to coordination of the oxygen atom with metal nanoparticles. The peak at 2350 cm^{-1} peak indicate C-H Stretching. The peak obtained at 1400 cm^{-1} is due to C-H bending²³. The peak at 1119 cm^{-1} is due to C-N bending. The peak around 1069 cm^{-1} is due to C-O stretching present in ring of polysaccharides²⁴. The peak around 595 cm^{-1} is due to metal carbon stretch²⁵. There is a slight change in frequency in the FTIR spectrum La/ Bi /Cu trimetal NPs of and La/ Bi /Cu /Chitosan Nanocomposites, which indicates the interaction between metal and O-H , C-N group of chitosan. These groups are responsible for the capping of trimetal nanoparticles.

X- Ray Diffraction Analysis (XRD)

X-ray diffraction (XRD) measurements were performed to confirm the desired crystal properties, phase composition, and orientation of the formed La/ Bi /Cu /Chitosan(4%(w/v))Nanocomposites. The XRD pattern for the sample is shown in Fig.3

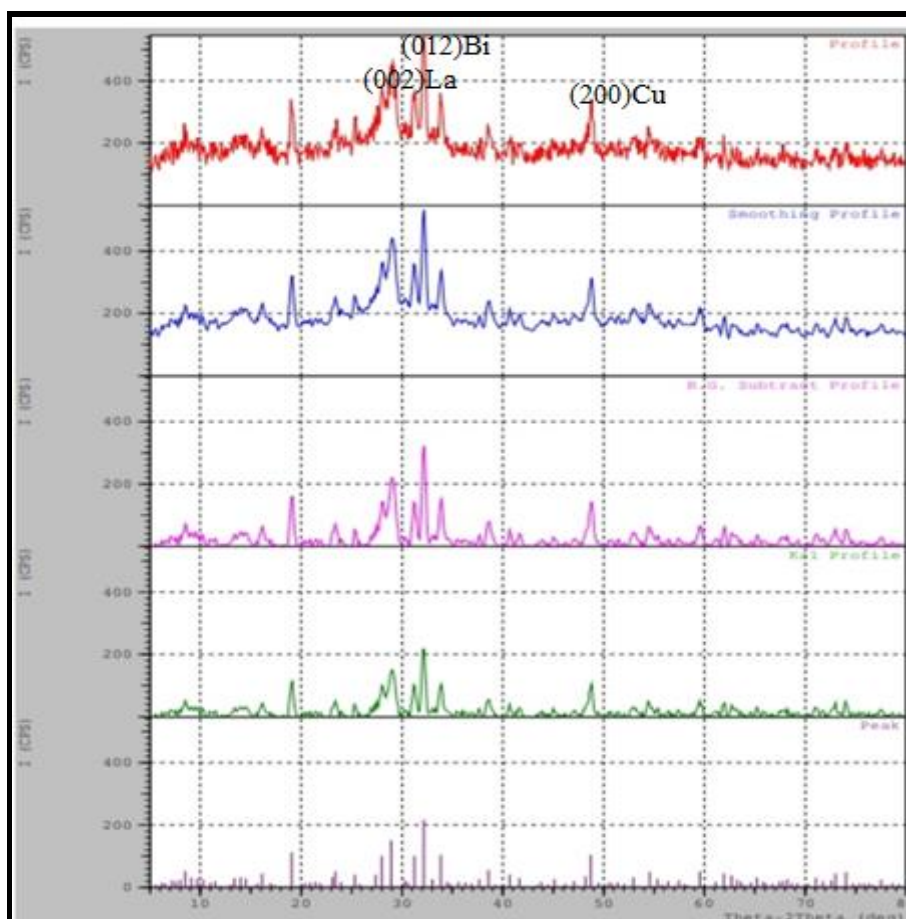


Fig. 3: XRD pattern of synthesized La/ Bi /Cu /Chitosan(4% (w/v)) Nanocomposites

The XRD pattern of synthesized La/ Bi /Cu /Chitosan (4% (w/v)) Nanocomposites shows peaks indices at (002) plane which indicates hexagonal crystals (La nanoparticle JCPDS no. 02-0607)²⁶. The (012) plane represent Rhombohedral crystals (Bi nanoparticles JCPDS Card No. 85-1331)²⁷. The plane (200) indicate the FCC crystals (Cu Nanoparticles JCPDS no. 04-0784)²⁸. From the indices, and comparison with the reported data, we conclude that the ternary nanocomposite has three different crystal structures with all three metals occupying the lattices in the crystals. The size of the La/Cu/Bi Chitosan (4% (w/v)) Nanocomposites calculated by using Debye- Scherrer's formula

$$d = \frac{K\lambda}{\beta \cos\theta}$$

Where d is the mean crystallite size, K is the constant (Shape factor) $K= 0.94$, λ is the Wavelength of X- ray ($\lambda = 0.154$ nm), β is the FWHM of the diffraction peak, and θ is the Bragg diffraction angle

Table 2: XRD data of La/ Bi /Cu /Chitosan(4% (w/v)) Nanocomposites

2 θ	θ	Cos θ	FWHM β	FWHM β (rad)	D (nm)
19.0568	9.5284	0.9862	0.4318	0.007513	18.3
31.2310	15.6155	0.9631	0.4600	0.008004	17.3
32.1482	16.0741	0.9609	0.4607	0.008210	17.9
33.8321	16.9116	0.9567	0.4909	0.008541	15.9
48.7321	24.3650	0.9109	0.4720	0.008210	18.5

Table 2 shows XRD data and the size of synthesized nanoparticles was found to be in the range of 15.9nm- 18.5nm.

Scanning Electron Microscopy

The surface morphology of the nanoparticles was studied by Scanning Electron Microscopy (SEM) analysis.

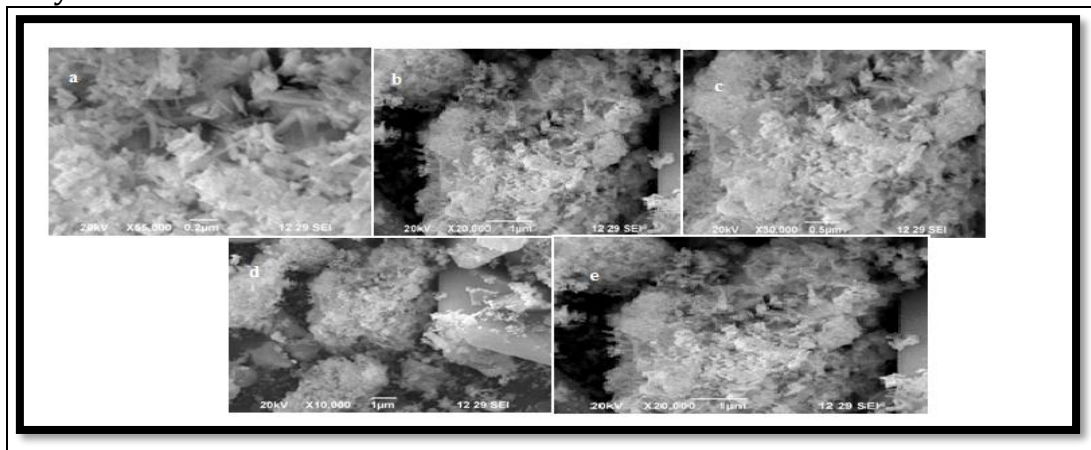


Fig. 4(a-e): SEM image of La/ Bi /Cu /Chitosan Nanocomposites at different concentration of ex was, wswss2qsqazwzwwzzaq(0.5%(w/v) , 1.0%(w/v) , 2.0%(w/v) , 3.0%(w/v) , 4.0%(w/v) ,) of Chitosan

The Fig.4 shows the SEM image La/ Bi /Cu /Chitosan Nanocomposite at different concentration of chitosan. It shows a needle like shape and it concurs with the results of XRD studies that it is crystalline. Some nanoparticles were found to be bigger in size; it may be due to the aggregation of the smaller ones.

Energy Dispersive X-Ray analysis (EDX)

Energy dispersive X-Ray analysis was carried out to find out the elemental composition of the synthesized La/ Bi /Cu /Chitosan(4% (w/v) Nanocomposites. The EDX shown in fig.5.

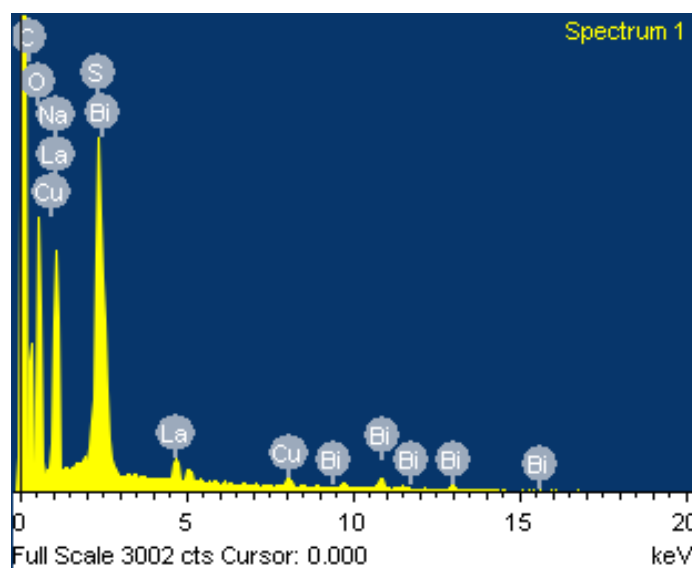


Fig. 5: EDX graph of La/ Bi /Cu trimetal NPs/Chitosan(4% (w/v))nanocomposites

EDAX graph of La/ Bi /Cu /Chitosan (4% (w/v)) Nanocomposite indicates the elemental composition of trimetal/chitosan nanocomposites. The sodium, carbon, and oxygen signals were most likely due to the reducing agent and polymer on the surface of the prepared nanoparticles. The other element S may be due to the presence of impurities.

Antifungal Activity:

Table: 3. Anti-fungal Activity of La/Bi/Cu/chitosan Nanocomposites

Fungal Strains	Sample Code Zone of inhibition (mm in diameter)		
	La/Bi/Cu/ChiosanNanocomposites (2)	Positive Control	Negative Control
<i>Aspergillusniger</i>	-	13	-
<i>Aspergillusflavus</i>	12	12	-
<i>Candida albicans</i>	10	12	-
<i>Aspergillusterreus</i>	- -	10	-

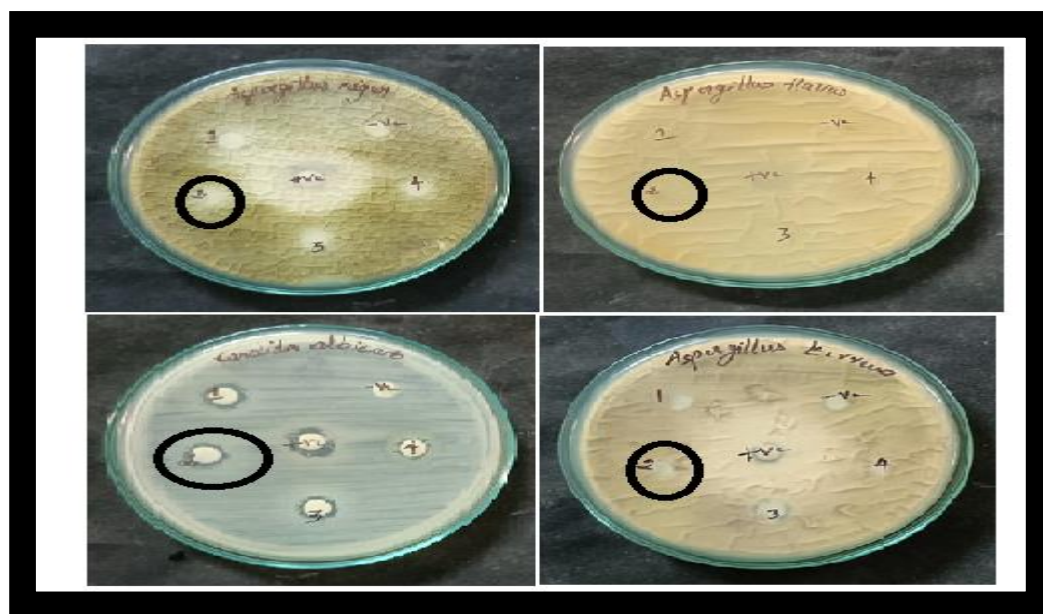


Figure: 6. Anti-fungal Activity of La/Bi/Cu/chitosan Nanocomposites

The Anti-Fungal activity of synthesized La/Bi/Cu /chitosan Nanocomposites was tested against the fungi such as *Aspergillus niger*, *Aspergillus flavus*, *Candida albicans* and *Aspergillus terrus sp.* are shown in Figure.6. The Zone of Inhibition of fungi strain shown in Table.3. This result showed was found inactive against two fungal strains namely *Aspergillus niger*, *Aspergillus terrus sp.*. The Nanocomposites showed remarkable antifungal activity in fungal stain *Aspergillus flavous* (12mm), *Candida albicans*(10mm) when compared positive control(12mm) .

Antibacterial Activity:

Table4. Zone of Inhibition of bacterial species(mm)

	Concentration ($\mu\text{g/L}$)	<i>Enterobacterclocae</i>	<i>Pseudomonas</i> VS1	<i>Bacillus</i> 1.3	<i>Bacillus</i> 8.3
chloramphenicol	1	2.6	3.5	3.7	3.7
La/Bi/Cu /chitosan nanocomposites	50	0.7	1.2	2.2	2
	100	0.9	1.5	2.6	2.4
	150	1	2	2.8	2.8

The antibacterial activity of La/Bi/Cu /chitosan nanocomposites was tested antibacterial activity against different bacteria such as two Gram negative bacteria (*Entero bacterclocae*, *Pseudomonas Vs1*) and two Gram positive bacteria (*Bacillus 1.3*, *Bacillus 8.3*) at different concentration (50-150 $\mu\text{g/L}$). The Zone of Inhibition of Gram negative and Gram positive bacteria shown in fig.7. The antibacterial activity of La/Bi/Cu chitosan Nanocomposites increases with increase the concentration of Nanocomposites shown in table3. . The concentration of Nanocomposites displayed adverse effect in antibacterial activity. This result showed La/Bi/Cu/chitosan Nanocomposites have good antibacterial activity against Gram positive bacteria when compared to Gram negative bacteria.

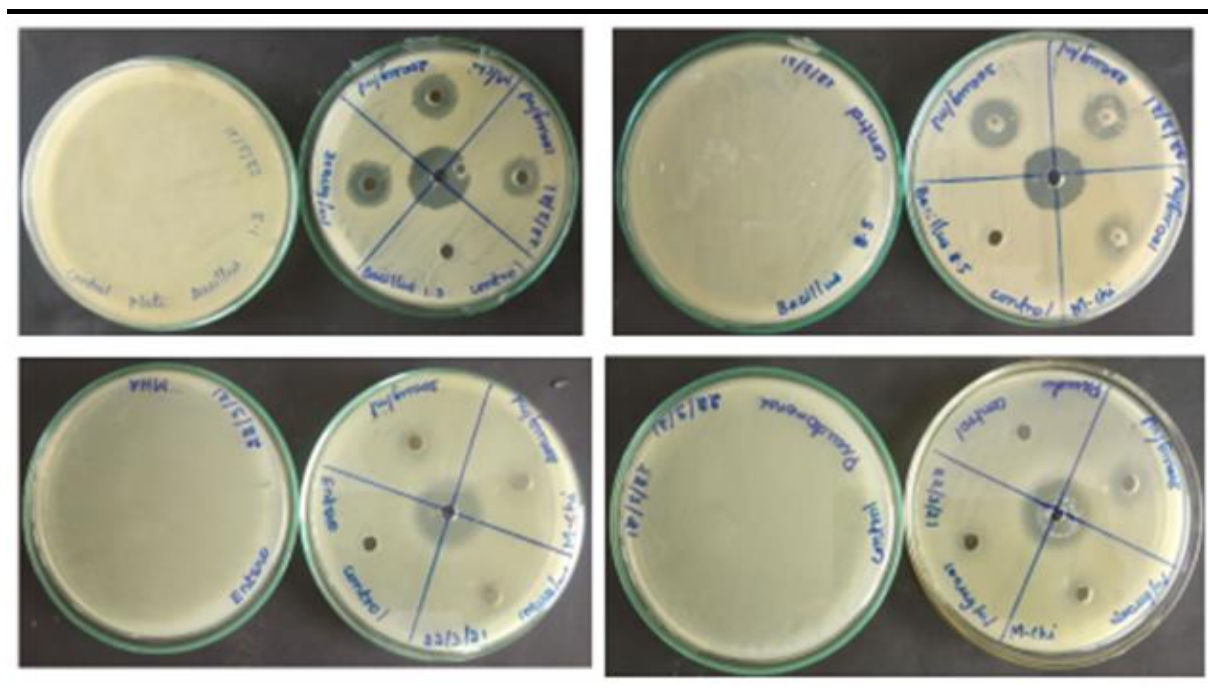


Figure: 7. Anti-bacterial Activity of La/Bi/Cu/chitosan Nanocomposites

Antioxidant Activity

Table. 5.DPPH assay for antioxidant activity

	Concentration (μg)	OD at 570nm	RSA %
Ascorbic acid	0.1	0.295333	3.485839
	0.2	0.289667	5.337691
	0.3	0.257667	15.79521
	0.4	0.213667	30.17429
	0.5	0.203	33.66013
La/Bi/Cu/Chitosan Nanocomposites	10	0.243667	25.4842
	20	0.234	28.44037
	40	0.231333	29.25586
	80	0.227	30.58104
	100	0.225333	31.09072

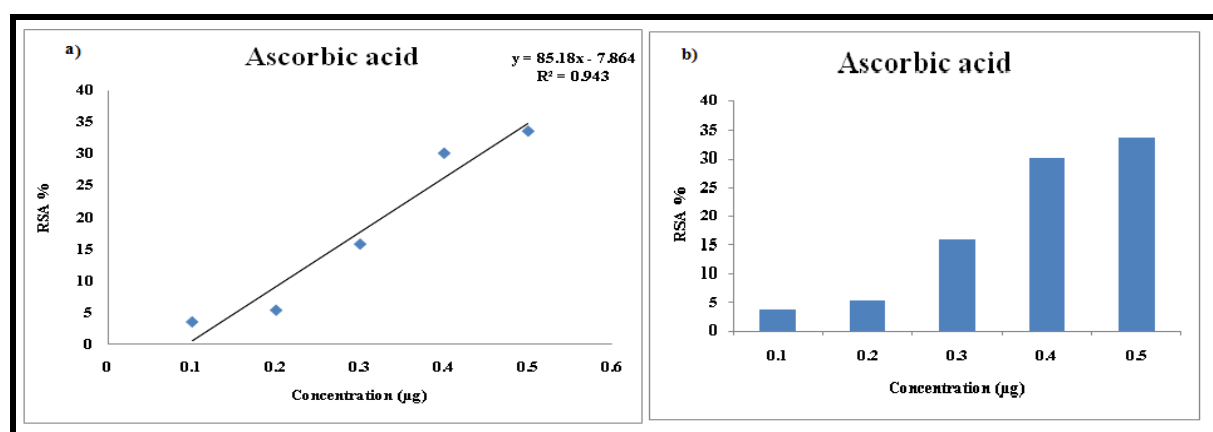


Fig. 8(a, b) DPPH radical scavenging activity of Ascorbic Acid

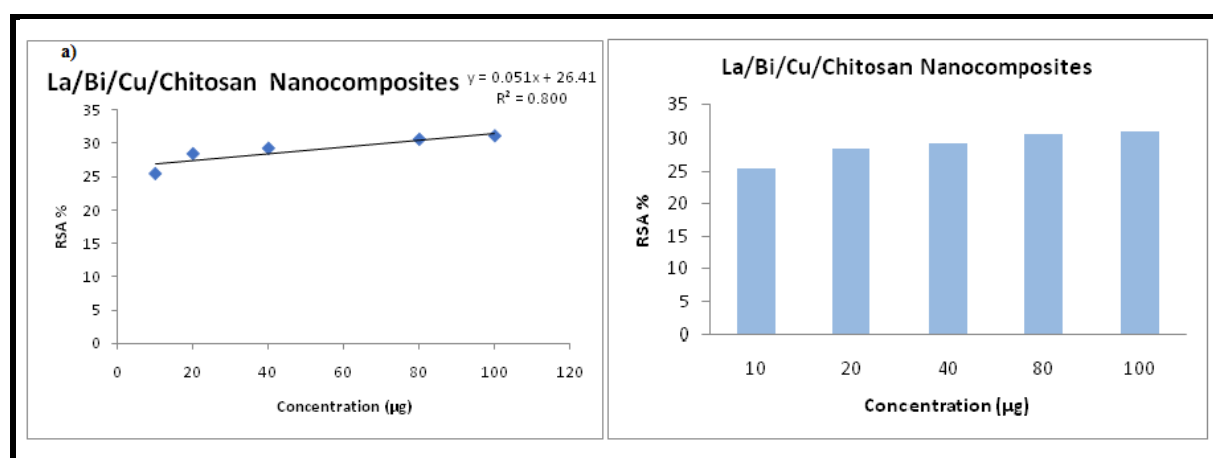


Fig. 9(a, b) DPPH radical scavenging activity of La/Bi/Cu /chitosan Nanocomposites

In vitro antioxidant activity of the synthesized La/Bi/Cu/Chitosan Nanocomposites was studied by analyzing DPPH radical scavenging activity at different concentrations from 10-100 $\mu\text{g/ml}$. DPPH (2,2-diphenyl-1-picryl-hydrazyl-hydrate) is a stable organic free radical that has been used for antioxidant assay. Table 5 shows DPPH scavenging activity of the synthesized La/Bi/Cu/Chitosan Nanocomposites at different concentrations. The varying concentration of the La/Bi/Cu/Chitosan Nanocomposites (10, 20, 40, 80 and 100 $\mu\text{g/ml}$) significantly scavenged DPPH by 25.4842, 28.44037, 29.25586, 30.58104, 31.09072% respectively.

Anticancer Activity

In vitro cytotoxic activity against HOS cell line at different concentrations was investigated. The anticancer activities of the La/Bi/Cu/Chitosan Nanocomposites were performed with different concentrations such (10, 20, 40, 60, 80 and 100 $\mu\text{l/ml}$). The anticancer activity of La/Bi/Cu trimetal nanoparticles against HOC cell line increased while in the concentration of La/Bi/Cu/Chitosan Nanocomposites. The results show the good cytotoxic activity against the cancer cells (Fig. 10). The concentration of La/Bi/Cu/Chitosan Nanocomposites plays an important role in the anticancer activity. The La/Bi/Cu trimetal nanoparticles are having the good results against HOS in that 100 μl show fine results followed by 80 μl , 60 μl , 40 μl , 20 μl and 10 μl . The lowest inhibitory action was observed from the concentration of 10 μl .

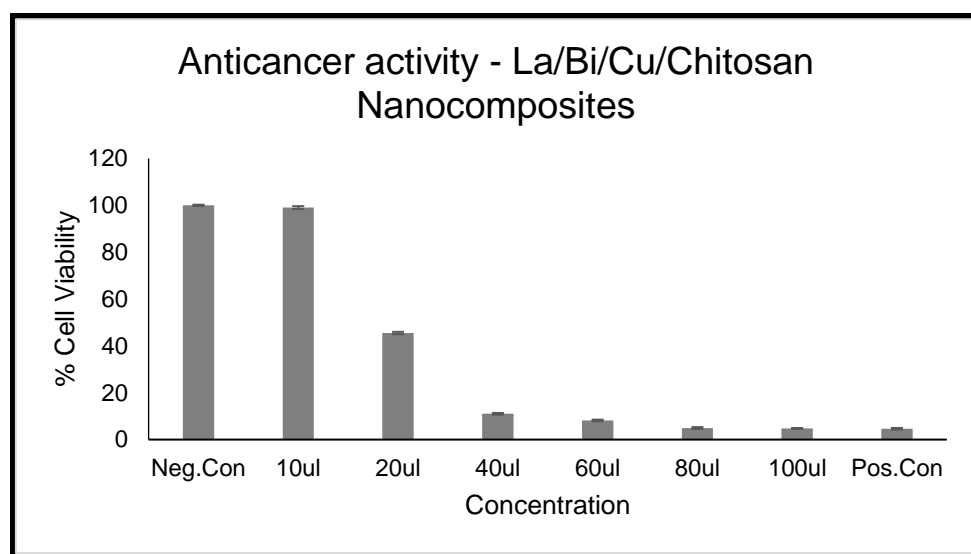


Fig. 13. Anticancer activity of La/Bi/Cu trimetal Nanoparticles against HOS cell line

Table.6 MTT assay on cytotoxic activity of La/Bi/Cu trimetal Nanoparticles against HOS cell.

Sample code: 2 (La/Bi/Cu/Chitosan Nanocomposites)					
Sample Concentration ($\mu\text{g/ml}$)	OD value I	OD value II	OD value III	Average OD	Percentage Viability
10 μl	1.776	1.754	1.765	1.765	99.02 ± 0.62
20 μl	0.808	0.821	0.803	0.810	45.46 ± 0.52

40 μ l	0.196	0.203	0.190	0.196	10.99 \pm 0.37
60 μ l	0.144	0.153	0.141	0.146	8.16 \pm 0.35
80 μ l	0.086	0.083	0.096	0.088	4.93 \pm 0.38
100 μ l	0.085	0.083	0.088	0.085	4.76 \pm 0.14

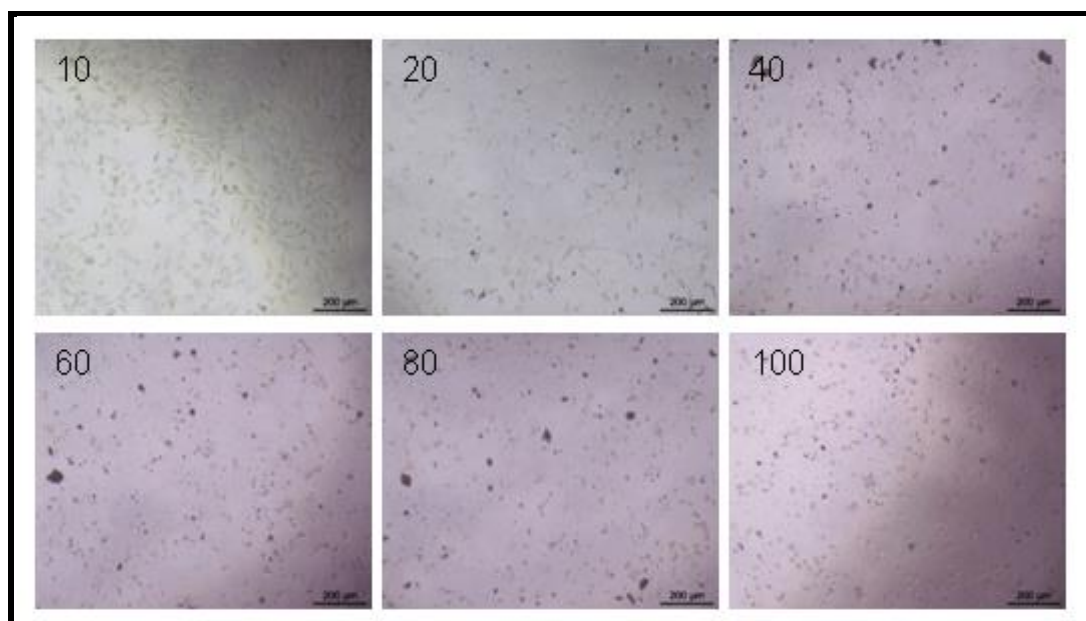


Fig.14. Microscopic image of Cytotoxic activity of La/Bi/Cu trimetal Nanoparticles against HOS cell line.

CONCLUSION

The La/ Bi /Cu /Chitosan Nanocomposites were successfully synthesized by using chemical method for synthesis. The Trimetal/Chitosan Nanocomposites were analyzed using UV-spectrophotometer, FTIR, SEM and EDAX, XRD. The La/ Bi /Cu /Chitosan Nanocomposites have biological activity such as antifungal, antibacterial, antioxidant and anticancer .

ACKNOWLEDGEMENT

The authors are thankful to Dr.C.Vedhi,Assistant Proessor,V.O.Chidambarm College, Thoothukudi for Providing nessasary research facilities.

CONFLICTS OF INTEREST

The authors declare no conflict of interest in present reearch work

REFERENCE

- 1Mark,J.E.; *Polym. Eng. Sci.*,**1996**,36,2905.
2. Carlson,G.; Gonsalves,K.E.;**1998**,49,769.
3. Akamatsu, K.; Takei,S.; Mizuhata, M.; Kajinami, A.; Deki, S.; Takeoka, S.; Fujii, M.; Hayashi,S.; Yamamoto, K.;*Thin Solid Films* ,**2000**,359,55.
4. Cole, D.H.; Shull, K.R.; Baldo, P.; Rehn, L.; *Macromolecules*,**1999**,32,771.
5. Kumar, R.V.; Elgamiel, R.; Diamant,Y.; Gedanken, A.; *Langmuir*,**2001**,17,1406.
6. Djokovic,V.; Nedeljkovic, J.M.; *Macromol. Rapid Commun.*,**2000**,21,994.

7. Yu, S.H.; Yoshimura, M.; Moreno, J.M.C.; Fujiwara, T.; Fujino, T.; Teranishi, R.; *Langmuir*, **2001**, *17*, 1700.
8. Croce, G.B.; Appetecchi, L.; Persi, B.; Scrosati, G.; *Nature*, **1998**, *394*, 456.
9. Guo, L.; Yang, S.; Yang, C.; Yu, P.; Wang, J.; Ge, W.; Wong, G.K.L.; *Chem. Mater.* **2000**, *12*, 2268.
10. Hamed, I.; Özogul, F.; Regenstein, J. M. , *Trends in Food Science & Technology*, **2016**, *48*, 40.
11. Deng, H.H.; Lin, X.; Liu, Y.H.; Li, K.L.; Zhuang, Q.Q. ; Peng, H.P.; *Nanoscale*. **2017**, *9*, 10292–300.
12. Crawford R.L.;. *New York (NY): John Wiley and Sons*, **1981**, 154.
13. Severyukhina, A.N.; Parakhonskiy, B.V.; Prikhozhenko, E.S.; Gorin, D.A.; Sukhorukov G.B.; Möhwald, H.; Yashchenok, A.M.; *ACS Appl. Mater. Interfaces*, **2015**, *7*, 15466–15473.
14. Kumar, M.N.V.R.; Muzzarelli, R.A.A.; Muzzarelli, C.; Sashiwa, H.; Domb, A.J.; *Chem. Rev.* **2004**, *1004*, 6017–6084.
15. Cao, C.; Xiao, L.; Liu, L.; Zhu, H.; Chen, C.; Gao, L.; *Appl. Surf. Sci.* **2013**, *271*, 105–112.
16. Lin, J.H.; Yan, F.; Hu, X.; Ju, H.; *J. Immunol. Methods*, **2004**, *291*, 165–174.
17. Kadib, El. ; *A. ChemSusChem* **2015**, *8*, 217–244.
18. Wei, D.; Ye, Y.; Jia, X.; Yuan, C.; Qian, W.; *Carbohydr. Res.* **2010**, *345*, 74–81
19. Mott, D.; Galkowski, J.; Wang, L.Y.; Luo, J.; Zhong, C.J. , *Langmuir* **2007**, *23*, 5740–5745.
20. Peniche, C.; Fernández, M.; Rodríguez, G.; Parra, J.; Jimenez, J.; Bravo, A.L.; Gómez, D.; San, R.J., *J. Mater. Sci. Mater. Med.* **2007**, *18*, 719–726
21. Esumi, K.; Takei, N.; Yoshimura, T.; *Colloid Surface B: Biointerf.* **2003**, *32*, 117.
22. Mahmoud, A.A.; Osman, O.; Eid, K.; Ashkar, E.A.; Okasha, A.; Atta, D.; Eid, M.; Aziz, Z.A.; Fakhry, A.; *Middle East Journal of Applied Sciences.* **2014**, *4(4)*, 816–824.
23. Vino, A.B.; Ramasamy, P.; Shanmugam, V.; Shanmugam, A. , *Asian. Pac. J. Trop. Biomed.* **2012**, *2*, S334–S341.
24. Wang, W.; Yu, W.; *Carbohydr Polym.* **2015**, *127*, 11–18.
25. de Abreu, F.R.; Campana-Filho S.P.; *Carbohydr Polym.*, **2009**, *75*, 214–221.
26. Djoudi, N.M.L.; Omari, M.; *EPJ Web Conf.* **2012**, *29 (00016)*, 1–9.
28. Lutful Kabir; Swapan Mandal, K. ; *International Journal of Modern Physics: Conference Series* , **2013**, *22*, 654–659.
27. Ezekiel Dixon Dikio, M.F.; *Chem. Sci. Trans.* **2013**, *2*, 1386–1394.
28. Abay, A.K.; Chen, X.; Kuo, D.H., *New J. Chem.*, **2017**, *41*, 5628–563